ISBN: 978-628-95207-4-3. ISSN: 2414-6390. Digital Object Identifier: 10.18687/LACCEI2023.1.1.1217

Methodology to estimate fuel`s exergy in SI engines using Otto cycles principles limited by the knock.

Juan Pablo Gómez Montoya [1], and Andrés Amell Arrieta [2]
[1] *Universidad Tecnológica del Perú, Lima-Peru.* jgomezmo@utp.edu.pe
[2] *Universidad de Antioquia, Medellín-Colombia.* andres.amell@udea.edu.co

Abstract: ***A novel methodology is proposed to estimate the exergy of liquid and gaseous fuels for spark ignition (SI) engines, based on the thermodynamics laws and two scientific methodologies, one for measurements of fuels methane number (MN), and other for estimation of gaseous fuels energy quality. Two engines were used 1) A CFR engine to measure fuel's critical compression ratio (CCR) and MN. 2) A hybrid diesel engine with a high compression ratio (CR) converted to SI using custom pistons for high turbulence intensity designed by CFD simulations, for biogas SI (BSI) combustion. In both engines, fuels with MNs ranging from 37 to 140 were used, biogases, methane, propane, and blends of biogas with methane/propane and hydrogen. The BSI engine combines diesel engines characteristics (high airflow inlet, and high combustion pressures) with SI engines characteristics (premixed combustion using SI for combustion phasing at the knocking threshold (KT)). The BSI engine was used to measure the fuel´s maximum electrical energy generation and thermal efficiency at the KT. Correlations between MN and research octane number (RON) were used to develop the methodology. Fuel´s exergy efficiency is estimated with fuel´s γ, hydrogen/carbon (H/C) ratio, and limited by fuel´s MN/RON. The methodology proposed correlates fuel´s exergy, fuel´s entropy, adiabatic flame temperature (T_{ad}), and fuel´s exergy efficiency for Otto cycles limited by the knocking.***

Keywords-- *Otto cycles; Knocking; Availability; Exergy; Entropy.*

I. INTRODUCTION

The maximum thermal efficiency of Otto cycles (η_{Otto}) for SI engines can be estimated using the principles proposed by Nicolaus Otto (1876), derived from the first and the second laws of thermodynamics applied to the Otto cycles process, which are: 1. Intake stroke is an isobaric process. 2. Compression stroke is an adiabatic and reversible (isentropic) process. 3. Heat release as a fast combustion, is an isochoric process at the top dead center. 4. Power stroke is an isentropic expansion. 5. Exhaust stroke consists of an isochoric process, and an isobaric process. η_{Otto} is determined using both the engine's CR and fuel's γ according to equation 1 [1]. A complete guide for calculating η_{Otto} is presented on the referred website [2]. η_{Otto} depends only on the temperatures and pressures at the beginning (T_A, P_A) and at the end (T_B, P_B) of the compression stroke, and not on how much heat is produced [2]. The actual cycles in SI engines differ from ideal Otto cycles, mainly because the combustion is not instantaneous and there is a formation of a flame front. Fuels like biogas and methane with high MN have high knocking resistance, allowing higher compression with higher T_B, and P_B, compared with fuels like gasoline or propane [3-5]. Equation 1 predicts that reducing T_A using air conditioning or increasing T_B using higher compression will increase η_{Otto}. Also, reducing P_A using partially throttle or increasing P_B using high CR and fuels with high MN will increase η_{Otto}. Then, fuels that get the highest temperature and pressure at the end of the compression stroke without knocking will have the highest theoretical η_{Otto}. Therefore, η_{Otto} and the knocking phenomenon hide the true operating limit for SI engines' performance.

$$\eta_{Otto} = 1 - \frac{1}{CR^{(\gamma-1)}} = 1 - \frac{T_A}{T_B} = 1 - \left[\frac{P_A}{P_B}\right]^{\frac{\gamma-1}{\gamma}} \quad \text{Eqn. 1.}$$

Technological development of internal combustion engines (ICE) has been based mainly on liquid fuels such as gasoline, kerosene, and diesel. Modern diesel engines employ a high CR (15-23:1) and are usually equipped with advanced turbocharging, exhaust after-treatment, exhaust gas recirculation (EGR), and common rail fuel injection systems [1,6,7]. SI engines employ a low CR (8-13:1) to avoid knocking when combusting highly reactive fuels with high laminar flame speeds (S_L), resulting in medium combustion pressure with high turbulent flame speed [1,8,9]. SI engines achieved the best results with liquid fuels with high RON because of the higher energy quality and knocking resistance [10].

Both SI and diesel engines achieve better performance using technologies that force greater charges of air and fuel into the engine, such as turbocharging, common rail, or turbo-compressors, and using intercooling systems for reducing air intake temperature [7,11-16]. From the thermodynamics point of view, diesel engines have better characteristics than SI engines because these achieve higher compression (higher T_B and P_B) by the higher CR and get higher combustion pressures. Modern SI engines are not designed according to Otto cycle principles to achieve maximum thermal efficiency because the knocking phenomenon is avoided using medium CR [17-23]. Commercial medium capacity (>200 kW) biogas engines could achieve the best thermal efficiencies close to 40% as reported by the manufacturers. But, for low capacity (<50 kW) efficient biogas engines are not commercially available at present, but these have been the subject of research in the last two decades, investigating strategies and configurations to optimize the performance of engines for biogas [24-35].

The objective of the present work proposes a methodology to estimate fuels exergy of liquid and gaseous fuels in SI engines according to the thermodynamics laws applied to the Otto cycles but using the knocking phenomenon as the engine limit. The novelty of the methodology is based on the combination of two scientific methodologies including data from various fuels tested in CFR engines. Also, own data from two engines are used to develop the methodology, a CFR engine to measure fuels MN and CCR, and a hybrid diesel engine for biogas (BSI engine), in both cases using the same fuels with MN between 37-140. The methodology presents a novel correlation between the fuel's octane, exergy, entropy, and flame temperature.

Digital Object Identifier: (only for full papers, inserted by LACCEI).
ISSN, ISBN: (to be inserted by LACCEI).

II. METHODOLOGY TO ESTIMATE EXERGY OF LIQUID AND GASEOUS FUELS IN SI ENGINES.

It is presented a unified methodology to estimate the exergy efficiency (η_{qT}) of liquid and gaseous fuels in SI engines. Before, was established a correlation to estimate the fuel's energy quality ($\overline{X_{f\,MN}}$) relative to methane by correlating certain physicochemical properties. Based on equations 9 and 15 of [36] provided the following correlations:

$$\overline{X_{fMN}} = E_{Dr}\, S_{Lr}{}^{0.262} T_{adr}{}^{0.368} H/C_r{}^{0.001} \gamma_r{}^{0.001} \quad \text{Eqn. 2.}$$

$$\overline{X_{fMN}} = \frac{ED_{CH4}}{ED_f}\left(\frac{SL_{CH4}}{SL_f}\right)^{0.262}\left(\frac{Tad_{CH4}}{Tad_f}\right)^{0.368}\left(\frac{H/C_{CH4}}{H/C_f}\right)^{0.001}\left(\frac{\gamma_{CH4}}{\gamma_f}\right)^{0.001}$$

In equation 3, is presented the maximum thermal efficiency in the function of fuel´s γ and MN (η_{qMN}) [37], it was derived from the classical η_{Otto}, replacing the engine CR with fuel's CCR, and fuel's CCR with fuel´s MN. More than 60 gaseous fuel blends were tested at the KT in the same CFR engine [17,20,38-44], according to Figure 11 in the appendix. η_{qMN} was found to be similar than η_{Otto}, η_{qMN} was estimated using the fuel's properties as engine limit, η_{Otto} only uses the CR of the engine and fuel's γ. Thus, η_{Otto} obscures information regarding the real engine limit of SI engines. η_{qMN} was defined as [37]:

$$\eta_{\mathbf{otto}} \approx \eta_{\mathbf{q\,MN}} = \mathbf{1} - \frac{\mathbf{1}}{\left[\mathbf{7.1635} * e^{\mathbf{0.00690} * \boldsymbol{MN}}\right]^{(\gamma-\mathbf{1})}} \quad \text{Eqn. 3.}$$

Previously was presented the estimated values of η_{qMN} and η_{Otto} versus fuel's MN for the fuel blends of the research [37]. η_{qMN} and η_{Otto} of each fuel were found to be similar, confirming the hypothesis that η_{Otto} can be assessed with η_{qMN} for gaseous fuels. In general, both η_{qMN} and η_{Otto} are increased using fuel blends with high γ and CCR. The intention of substituting CR with MN is to attain insight into the best fuel's operating conditions, informing engine design according to the ideal Otto cycles process, to get the highest thermal efficiency possible based on the fuel's physicochemical properties, with engine output power limited by fuel's knocking resistance. SI engines could be designed by considering the fuel's exergy at the KT, derived from the Otto cycles principles, and the fuel's physicochemical properties given by the chemical composition, and limited by its knocking resistance. A new approach to engine design is proposed: first, the fuel must be studied, identifying its physicochemical properties energy density (E_D), S_L, T_{ad}, H/C ratio, γ, and MN/RON, then, this information is used to estimate η_{qMN} or η_{qRON}, $\eta_{qH/C}$, and η_{qT}. Finally, the engine geometry and operating conditions are selected, such as CR, piston head design, combustion turbulence intensity, equivalence ratio, ST, and engine speed.

Fuel´s exergy ($\overline{X_f}$) is defined as the maximum portion of the chemical availability that could be converted into useful work. For SI engines applying the thermodynamics laws for the ideal Otto cycles results that the maximum thermal efficiency is $\eta_{\mathbf{Otto}}$. Also, the fuel´s exergy (η_{qT}) could be estimated with the thermal efficiency averaged between η_{qMN} and $\eta_{qH/C}$, calculated at the engine limit measuring the knocking threshold (KT) and fuel´s CCR, as follows [37],

$$\overline{X_f} = A_{c-f} * \eta_{\text{Otto}} \approx A_{c-f} * \eta_{\text{q T}} \quad \text{Eqn. 4.}$$

Then, the new methodology to estimate the exergy of liquid and gaseous fuels in SI engines proposes the calculation of a total exergy efficiency (η_{qT}). It considers two effects: the fuel's chemical availability to produce work based on the fuel`s chemical composition, limited by the fuel´s combustion instabilities by the knocking phenomenon (quantified with MN or RON). η_{qT} is defined for gaseous and liquid fuels as,

$$\eta_{\mathbf{qT}} = \frac{\eta_{q\frac{H}{C}} + \eta_{\mathbf{q\,MN}}}{\mathbf{2}}, \eta_{\mathbf{qT}} = \frac{\eta_{q\frac{H}{C}} + \eta_{\mathbf{q\,RON}}}{\mathbf{2}} \quad \text{Eqn. 5.}$$

Fuel´s exergy for SI engines is proposed to be estimated as the chemical availability converted into useful work according to the thermodynamics laws applied to ideal Otto cycles, and limited by engine performance at the KT (Eqn.4). It is proposed that $\overline{X_f}$ can be estimated using η_{qT} or η_{Otto} for SI engines. Kubesh and King developed two correlations between the motor octane number (MON), the reactive fuel's H/C ratio, and between MON and MN [45]. These correlations provide practical methods for determining equivalent MON for gaseous fuels, and provides a significant insight into the effects of heavy hydrocarbons on the fuel´s MON. The MON and MN were measured for twelve fuel blends to determine the correlations between MN, MON, and H/C ratio,

$$\text{MN} = 1.445 * \text{MON} - 103.42 \quad \text{Eqn. 6.}$$

$$\text{MON} = -406.1 + 508.0 * \frac{\text{H}}{\text{C}} - 173.5 * \left(\frac{\text{H}}{\text{C}}\right)^2 + 20.2 * \left(\frac{\text{H}}{\text{C}}\right)^3 \quad \text{Eqn. 7.}$$

This equation can be expressed in exponential terms as,

$$MON = \mathbf{50.022} * \boldsymbol{e}^{\mathbf{0.2381} * \boldsymbol{H/C}} \quad \text{Eqn. 8.}$$

Replacing Eqn. 6 in Eqn. 3 gives the maximum thermal efficiency as a function of MON (η_{qMON}),

$$\eta_{\mathbf{qMON}} = \mathbf{1} - \frac{\mathbf{1}}{\left[\mathbf{7.1635} * e^{(\mathbf{0.009971} * \boldsymbol{MON} - \mathbf{0.713598})}\right]^{(\gamma-\mathbf{1})}} \quad \text{Eqn. 9.}$$

Other previous research [46-48] tested twelve liquid fuels in CFR engines, giving the following relationship:

$$\text{MON} = 0.894 * \text{RON} \quad \text{Eqn.10.}$$

Substituting Eqn. 10 in Eqn. 9 gives the maximum thermal efficiency as a function of RON (η_{qRON})

$$\eta_{\mathbf{qRON}} = \mathbf{1} - \frac{\mathbf{1}}{\left[\mathbf{7.1635} * e^{(\mathbf{0.008914} * \boldsymbol{RON} - \mathbf{0.713598})}\right]^{(\gamma-\mathbf{1})}} \quad \text{Eqn.11.}$$

Substituting Eqn. 8 in Eqn. 9 gives maximum thermal efficiency as a function of the fuel's H/C ratio ($\eta_{qH/C}$),

$$\eta_{\mathbf{qH/C}} = \mathbf{1} - \frac{\mathbf{1}}{\left[\mathbf{7.1635} * e^{(\mathbf{0.498744} * e^{\mathbf{0.2381} * \boldsymbol{H/C}} - \mathbf{0.713598})}\right]^{(\gamma-\mathbf{1})}} \quad \text{Eqn. 12.}$$

The double exponential in Eqn. 12 allows a quantum analysis of the correlation between fuel´s chemical composition and exergy efficiency, according to the Otto cycles principles.

Specifically, in the BSI engine the fuel´s exergy estimation is used to measure the correlation between E_{Emax} and its thermal efficiency (η_q) for electrical energy (EE) generation at the KT (exergy definition by the BSI engine), according to the fuel´s exergy efficiency definition ($\boldsymbol{\varepsilon}$) [49]:

$$\varepsilon = \frac{Availability\_out}{Availability\_in} = \frac{Exergy}{A_{c-f}} = \frac{Output\ power\ or\ EE}{Energy\ in\ mass\ flow}$$

$$\varepsilon \approx \eta_q = \frac{Exergy\ out\ (EE \cap KT)}{Availability\ in} = \frac{E_{E\,max}}{A_{c-f}}\ @60Hz \cap KT \quad \text{Eqn. 13.}$$

Using the general definition of fuel´s entropy (S_f) for SI engines, the heat release (Q_{in}) is the fuel´s chemical availability ($\boldsymbol{A_{c-f}}$) for a complete combustion process with a temperature source (T_f). Then, for the BSI engine, to generate EE_{max} operating at the KT with $\eta_{\boldsymbol{q}}$, and for the minimum entropy is used the maximum fuel´s temperature for the combustion process, using the fuel´s adiabatic flame temperature (T_{ad}), and including Eqn. 13,

$$\boldsymbol{S_f} = \frac{\boldsymbol{Q_{in}}}{\boldsymbol{T_f}} = \frac{\boldsymbol{A_{c-f}}}{\boldsymbol{T_{ad}}} = \frac{\boldsymbol{E_{Emax}}}{\boldsymbol{T_{ad}}*\boldsymbol{\eta_q}} @\boldsymbol{60Hz} \cap \boldsymbol{KT} \qquad \text{Eqn. 14.}$$

Combining equations 14 and 4 gives the fuel´s exergy for SI engines, written in terms of fuel´s entropy, T_{ad}, η_{Otto}, or η_{qT}.

$$\overline{\boldsymbol{X_{f\,SI}}} = \boldsymbol{\eta_{Otto}} * \boldsymbol{S_f} * \boldsymbol{T_f} \approx \boldsymbol{\eta_{qT}} * \boldsymbol{S_f} * \boldsymbol{T_{ad}} \qquad \text{Eqn. 15.}$$

Besides replacing the last part of Eqn. 15 with Eqn. 14 could permit finding a relation between fuel´s exergy, and E_{Emax} operating the BSI engine at 60Hz and at the KT, which is proportional to the ratio between the exergy efficiency and generating efficiency for EE generation.

$$\overline{\boldsymbol{X_f}} = \frac{\boldsymbol{\eta_{qT}}}{\boldsymbol{\eta_q}} * \boldsymbol{E_{E\ max}} @\boldsymbol{60Hz} \cap \boldsymbol{KT} \qquad \text{Eqn. 16.}$$

Equation 15 includes the experimental findings found in the global research, that are in accordance with the laws of thermodynamics and the engine performance:

- Higher octane fuels get higher output power or E_{Emax}.
- Gaseous fuels with higher entropy than liquid fuels achieve higher CCR and higher thermal efficiency.
- Higher combustion temperature increases availability but is limited by the knocking tendency.
- Higher entropy conditions (high pressure and turbulence) allow higher exergy using high octane fuels like biogases.
- This is a new expression that allows the design of SI engines according to the laws of thermodynamics, to select the operating conditions according to the fuel´s chemical composition and its knocking resistance.

The main fuel properties, BSI and CFR engine experimental setup, analysis of errors, uncertainty, and repeatability have been fully presented previously in the paper series [36-43].

There are some recent studies that present exergy analysis for SI engines. Research presents an energy-exergy analysis and sustainability assessments of ketone-gasoline blends and were compared with gasoline; the 10% blended ketones fuels have comparable energy-exergy and sustainability assessment to that of commercial gasoline [50]. An energy and exergy analysis was done utilizing combinations of gasoline, natural gas, and methanol; with an increase in torque values, all fuel types' first and second-law efficiencies increased [51]. In other research, are presented the effects of two different modes on the energy and exergy balance of a SI engine working under lean-burn conditions; the results show that the cooling water takes 39.40% of the fuel energy; the exergy destruction occupies 56.12% of the fuel exergy [52]. An energy and exergy analysis of a hydrogen-fueled four-stroke SI engine is presented varying the CR; the increase in CR yields a decrease in exergy destruction [53]. Research presents a model extended to include exergy terms complementing the first-law analysis for a variable CR gasoline engine; it is presented an estimate of the generation of entropy during this process. History diagrams of the exergy and entropy including the turbulent entrained mass, reveal the influence of the entrained mixture mass exergy as the cylinder-content related exergy shifts too in the same direction as identified also by considering the temperature and chemical species histories in the burned zone [54]. A research paper on energy and exergy characteristics contributes to a deeper understanding of the performance of an ethanol-fueled SI engine. The engine's thermal efficiency and combustion phasing are evaluated for knock-limited operation; entropy generated through combustion is discussed to identify the relationship between exergy destruction. The exergy destruction by the in-cylinder process can decrease the exhaust exergy [55]. According to these papers, there is a research gap to correlate octane, exergy, and entropy for fuels in SI engines.

III Experimental Results of the Methodology

Figure 1 presents the values of the measured E_{Emax} in the BSI engine, and the estimated energy quality ($\overline{X_{f\,MN}}$) versus the fuel's MN. $\overline{X_{f\,MN}}$ is defined as the ratio of certain physicochemical properties of the tested fuel relative to methane according to equation 2. E_{Emax} increases with the rise of both MN and $\overline{X_{fMN}}$.

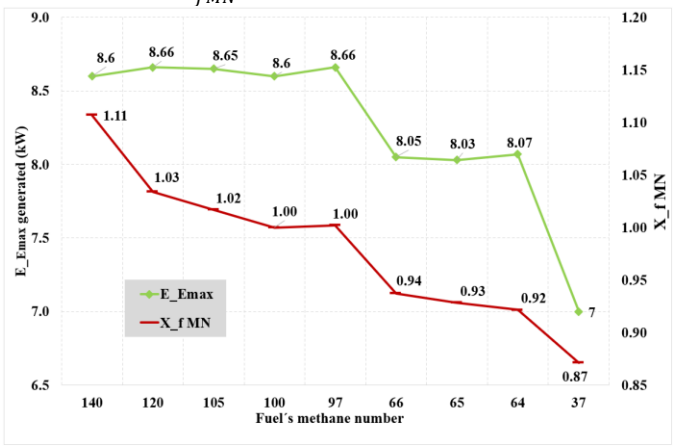

Figure 1 BSI engine data: E_{Emax} and X_{fMN} vs. fuel's MN.

Methane is established with $\overline{X_{f\,MN}} = 1$ as the reference fuel. Fuels with $\overline{X_{f\,MN}} > 1$ are biogases with MN>105 with low E_D, low S_L, low T_{ad}, low H/C ratio, and high γ. Biogases have high exergy because of the good balance of physicochemical properties and high knocking resistance, but biogases require both high combustion pressure and high turbulence intensity during combustion. Increased biogas CO_2 content resulted in exponential growth of knocking resistance [44], and higher $\overline{X_{f\,MN}}$. $\overline{X_{f\,MN}} > 1$ represents higher fuel energy quality for electrical energy generation relative to methane operating at the KT. Biogas MN140 with $\overline{X_{f\,MN}} = 1.107$ had a high E_{Emax} (8.60 kW) operating at high pressure with high turbulence intensity, while biogas MN120 with $\overline{X_{f\,MN}} = 1.102$ had a high E_{Emax} (8.66 kW) but operating with medium turbulence intensity. Fuels with $\overline{X_{f\,MN}} < 1$ have low MN, high E_D, high S_L, high T_{ad}, low H/C, and low γ. Fuels with $\overline{X_{f\,MN}} < 1$ have

medium fuel energy quality for electrical energy generation at the KT relative to methane, requiring medium or low turbulence intensity and low compression pressures during combustion.

Figure 2 presents E_{Emax} and η_{qMN} versus the fuel's MN in the BSI engine. There is a correlation between E_{Emax} concerning η_{qMN} at the KT, which is the base of the methodology for estimating exergy efficiency. η_{qMN} is proposed to estimate the maximum thermal efficiency in conformity with Otto cycles principles while considering the KT as the engine limit. Propane MN37 exhibited the lowest η_{qMN} and the lowest E_{Emax} due to its high knocking tendency given by its high S_L, high T_{ad}, and high E_D. Conversely, biogas MN140 exhibited the highest estimated η_{qMN}, due to its high knocking resistance given by its low S_L, low T_{ad}, and low E_D. Biogas MN140 achieved an E_{Emax} (8.60 kW) using high turbulence, close to the highest output power (8.66 kW@60Hz) of the BSI engine for EE generation. Methane MN100 is the reference fuel for measuring the energy quality of gaseous fuels due to it has the highest H/C ratio (4/1), it got E_{Emax} (8.60 kW) close to the highest EE due to its good balance between γ, S_L, T_{ad}, E_D, and MN. Besides, methane has no CO_2 content in its chemical composition and had lower exhaust mass flow with lower heat losses, which allows it to achieve the best η_q (30.2%) in the BSI engine to EE generation. Fuels with MN>97 have η_{qMN} >55.8%, indicating that fuels with high knocking resistance have high exergy efficiency, as these fuels can operate at high combustion pressures obtainable in high CR SI engines. In contrast, fuels with MN <66 have η_{qMN} <46%, indicating that fuels with a high knocking tendency have low exergy efficiency, and must be used with medium combustion pressure and CR in SI engines with low turbulence intensity. Propane MN37 with η_{qMN} (24.6%) has a high knocking tendency and must be used in medium CR (9-11) SI engines, due to propane having a high S_L, low turbulence intensity is enough to reach high turbulent flame speeds.

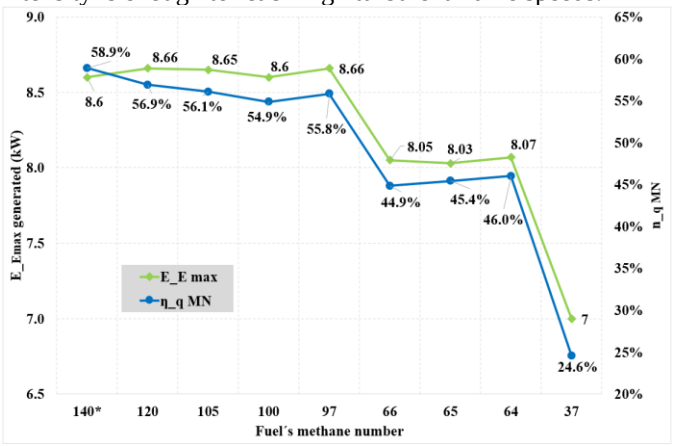

Figure 2 BSI engine data: E_{Emax} and $\eta_{q\ MN}$ vs. fuel's MN.

Figure 3 presents E_{Emax} and $\eta_{q\ H/C}$ versus the fuel's MN. Methane has the highest $\eta_{qH/C}$ due to the highest H/C ratio, allowing it to get the highest η_q in the BSI engine to E_{Emax} by chemical composition. Fuels with MNs <97 have a high knocking tendency, with lower H/C ratios, leading to reduced CCR, MN, and E_{Emax}. Fuels with MNs >97 have high knocking resistance due to their CO_2 content, with lower H/C ratios leading to greater CCR, MN, and E_{Emax}. Fuels with MNs >100 usually contain CO_2, increasing their MN and CCR but increasing exhaust gases and heat losses, leading to reduced thermal efficiency. For biogas MN120, medium turbulence intensity was enough to reach the limit of 8.66 kW, while biogas MN140 required greater turbulence intensity to release the maximum energy to reach the highest output power at the KT. Biogases with MN>140 would require even greater turbulence intensities as well as CR to release the fuel's energy to attain the best engine operation at the KT. The methodology presented proposes that the combustion chamber geometry of the piston heads must be selected according to the fuel's chemical composition, MN, and S_L. Also, Fuels with MN>97 operate best with lean equivalence ratios (near stoichiometric 0.90-0.95) due to their high CO_2 content, which reduces the E_D of the mixture, the low E_D of the biogas is enough to reach low T_{ad} with low NOx emissions, as a strategy to achieve clean combustion. While fuels with MN<97 operate best with leaner equivalences ratios (0.80-0.90) and is required both low CR and turbulence intensities for reducing knocking tendency, and advanced ST for improving the combustion phasing. Fuels with MN<97 have a high T_{ad}, which is reduced by leaner combustion, decreasing T_{ad} to reduce NOx emissions.

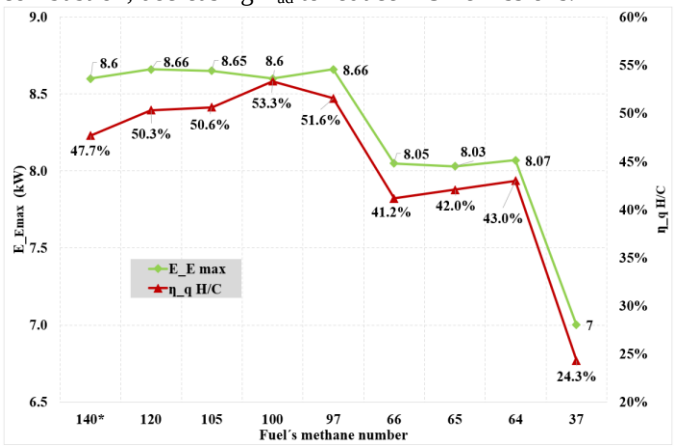

Figure 3 BSI engine data: E_{Emax} and $\eta_{q\ H/C}$ vs. fuel's MN.

Figure 4 presents E_{Emax} and η_{qT} versus the fuel's MN in the BSI engine. η_{qT} is used in the methodology proposed to estimate the exergy efficiency of gaseous and liquid fuels in SI engines. $\eta_{qH/C}$ measures the fuel's availability to produce work by the fuel's chemical composition limited by η_{qMN} which measures the thermal efficiency according to the Otto cycles principles limited by the knocking resistance (fuel's MN). η_{qMN} was shown to have similar values to η_{Otto}. However, η_{qT} exhibits a better fit to E_{Emax} estimation as was compared with η_{qMN} or $\eta_{qH/C}$, presented in Figs. 2 and 3, which is according to the methodology presented and the hypothesis for evaluating the exergy efficiency of gaseous fuels. Methane exhibited the best η_{qT} =54.1% serving as the reference fuel due to its highest H/C ratio and the good balance between knocking resistance and physicochemical properties. Fuels with MN>97 have similar

values of η_{qT} (53.3% - 54.1%) indicating a comparable exergy efficiency but requiring the correct turbulence intensity and pressure for the combustion process to get optimal performance and exergy release. Medium turbulence intensity is required for fuels with a MN between 97 and 120; for biogas, MN140 is required a high turbulence intensity to increase the turbulent flame speed due to its low S_L. Fuels MN64-66 had lower η_{qT} values (43% - 44.5%) due to their high knocking tendencies. Propane MN37 had the lowest η_{qT} (24.5%) due to its low H/C ratio and knocking resistance. Fuels with MN<66 require low turbulence intensity to achieve high turbulent flame speed due to their high S_L, and require low CR (9-11).

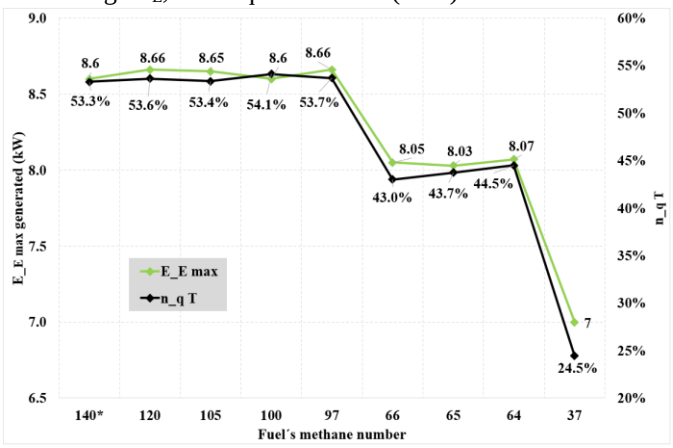

Figure 4 BSI engine data: E_{Emax} and $\eta_{q\,T}$ vs. fuel's MN.

Figure 5 presents $\eta_{qH/C}$, η_{qMN}, and η_{qT} versus the fuel's MN. The methodology proposes that η_{qT} is defined as the average of η_{qMN} and $\eta_{qH/C}$ for estimating exergy efficiency as fuel's availability to produce work and limited by the knocking phenomenon, besides, fuel´s chemical composition is an indicator of energy quality for gaseous fuels, comparing certain physicochemical properties relative to methane. For propane and methane, $\eta_{qH/C}$, η_{qMN}, and η_{qT} are very close to each other in values, due to being pure substances. Conversely, fuels MN97, MN105, MN120, and MN140 exhibit more varied values of $\eta_{qH/C}$ and η_{qMN}. The maximum thermal efficiency to E_{Emax} is better represented and estimated by the proposed exergy efficiency η_{qT}. In general, η_{qMN} was like η_{Otto}, even with similar values, increasing with CCR, but both estimated higher thermal efficiency than those given by $\eta_{qH/C}$ *and* $\eta_{qH/C}$. Finally, η_{qT} allows a close estimation of the maximum thermal efficiency for E_{Emax} at the KT in the BSI engine, as was presented in Fig. 4, it can better predict the engine performance relating to pressure, temperature, turbulence, and knocking, also taking into account the fuels chemical composition (H/C). Fuels with MN>97 had similar η_{qT} (53.3%-54.1%), and similar E_{Emax} (8.60 kW-8.66 kW), then fuels with MN>97 have similar exergy, but fuels with MN>120 require high turbulence intensities to achieve the maximum E_{Emax} at the KT.

Figure 6 presents E_{Emax} measured at the KT and the estimated η_{Otto} versus the fuel's MN. η_{Otto} was estimated using fuel's γ and fuel´s CCR measured in the CFR engine. E_{Emax} was measured using the knocking threshold as engine limit to understand the physics and chemistry of gaseous fuel combustion in SI engines. The highest η_{Otto} was for biogas MN140 as it has the highest CCR (18:1), while it has a low H/C ratio and low $\eta_{qH/C}$. Biogas and methane have similar η_{qT} (53.3% and 54.1%) with comparable values of E_{Emax} (8.6 kW). Fuels with MN>97 had comparable η_{Otto} (55.5%-58.3%) while MN64, MN65, and MN66 had similarly lower η_{Otto} (44.6%-45.7%) due to their low CCR. Propane MN37 had the lowest η_{Otto} (24.6%) due to its low knocking resistance and CCR.

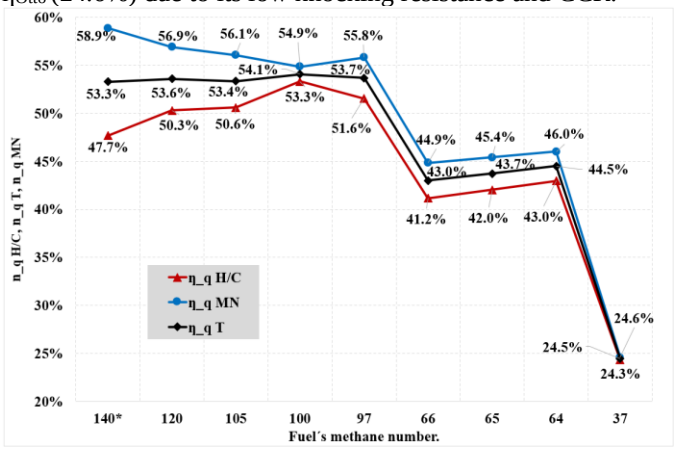

Figure 5 BSI engine data $\eta_{qH/C}$, η_{qMN}, η_{qT}, vs. fuel's MN.

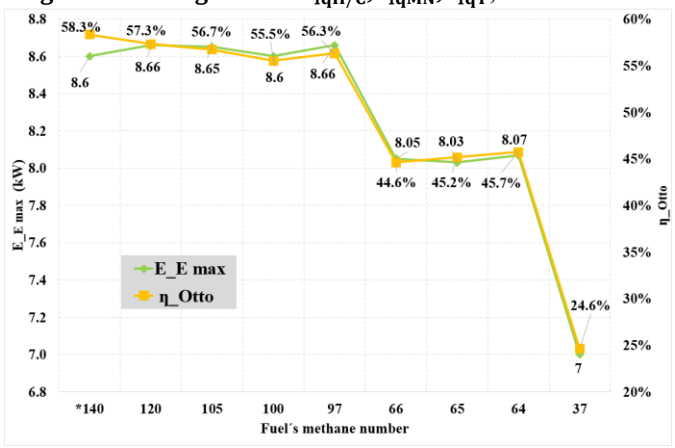

Figure 6 BSI engine data: E_{Emax} and η_{Otto} vs. fuel's MN.

Data in figures 4 and 6 are used for the validation of the proposed methodology, which has the hypothesis that $\eta_{Otto} \approx \eta_{qT}$, which correctly estimates the tendency and correlation between E_{Emax} and fuel`s MN. But $\eta_{qT}$ predicts lower efficiencies than $\eta_{Otto}$ due to the knocking phenomenon limit and fuel`s chemical composition (H/C ratio), on average 2.3% less for the fuels analyzed.

Figure 7 presents the measured thermal efficiency η_q in the BSI engine for E_{Emax} generation at the KT, and the estimated η_{qT} and η_{Otto} versus the fuel's MN. Methane got the highest η_q due to the highest H/C ratio. Biogases have lower η_q than methane because of the high CO_2 content and greater mass flow, which increased heat losses and reduced thermal efficiency, it also

increased knocking resistance but reduces the H/C ratio and $\eta_{qH/C}$. Methane has better η_q than propane because of the higher knocking resistance which permits to get higher E_{Emax} with better η_q at higher compression pressures. Fuel blends of biogas with propane have on average a low η_q of 27.6% because of the power derating (0.6 kW) for these blends due to the high knocking tendency of the propane.

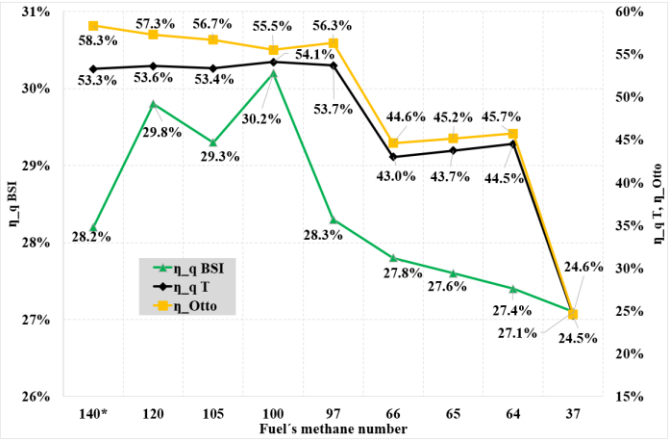

Figure 7 n_q, n_{qT}, and n_{Otto} vs. fuel's MN.

Figure 8 presents the estimated minimum fuel entropy in the BSI engine at the KT for EE generation, and η_{Otto} vs. fuel´s MN. Biogas MN140 has greater entropy than methane MN100 because to reach a similar E_{Emax} of 8.6 kW at the KT, biogas required a higher mass flow, and turbulence intensity for combustion, also biogas has lower T_{ad} and η_q. Additionally, the heat losses are higher for biogas because of the greater exhaust gases mass. In general fuels with both high knocking resistance and high H/C ratio have high exergy efficiency and high values of η_{Otto}. Propane MN37 had lower entropy to EE generation in the BSI engine because of the low E_{Emax} of 7.0 kW at the KT, and the high T_{ad}; also, propane has lower entropy than methane because the C_3H_8 molecules are larger than the CH_4 molecules, then the hydrogen and carbon atoms could be located probabilistically more easily. According to the methodology presented, fuels like biogases with high entropy in their chemical composition have high exergy at the KT because of the high γ, low T_{ad}, low S_L, low E_D, and high knocking resistance despite the low H/C ratios. It agrees with Otto cycles principles and the thermodynamics laws because biogases can be higher compressed (with higher T_A and P_A) for combustion. Figure 9 presents the fuel´s entropy in the BSI engine at the KT for EE generation, and the fuel´s exergy efficiency vs. the fuel´s MN, which presents a similar shape and tendency as Figure 8. Fuels with high MN have high entropy due to these fuels have greater availability to produce work because of their chemical composition related to the fuel´s γ, H/C ratio and MN because of the high knocking resistance, which permits a combustion process with high turbulence intensity, and compression pressure. For the system inside the cylinder of the engine, at high compression pressures and turbulence intensity for combustion, the fuel´s exergy and the fuel´s entropy are also high. In general, according to equation 15, fuels that get the highest entropy at the KT have the highest exergy in SI engines. For similar reasons, gases have greater entropy than liquids, resulting that, gaseous fuels have greater exergy than liquid fuels, and greater exergy efficiency according to Otto cycles principles.

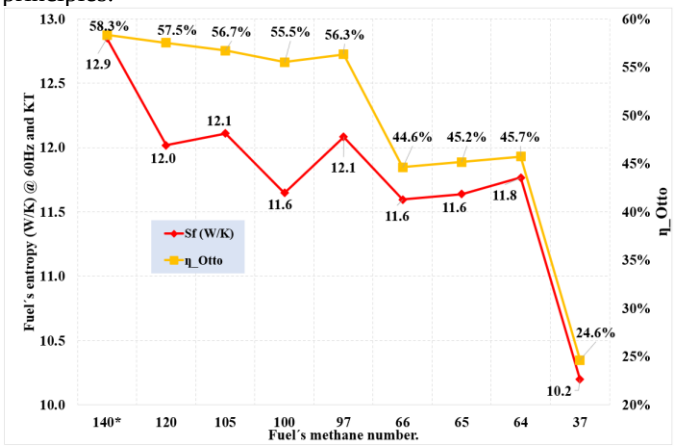

Figure 8 Fuel´s entropy and η_{Otto} vs. fuel´s MN.

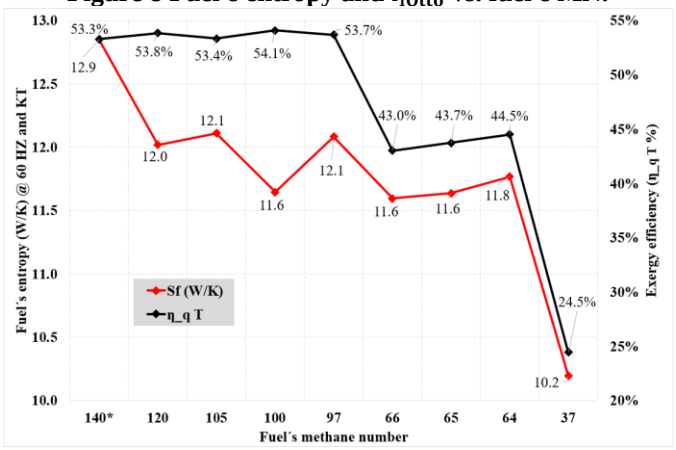

Figure 9 Fuel´s entropy and η_{qT} vs fuel´s MN.

Results of the methodology to estimate exergy efficiency of liquid and gaseous fuel in SI engines.

Table 1 in the appendix presents the data used for estimating the exergy efficiency of some liquid and gaseous fuels. The present research tested gaseous fuels with MNs between 37-140, also, using Eqns. 6 and 10 are estimated the equivalent RON and MON. Besides, test data from other research in the same type of CFR engines were used for eight liquid fuels (gasoline) with RONs between 0-109, also their equivalent MON and MN~ were calculated using these equations. Then, the maximum thermal efficiency limited by knocking resistance could be estimated in terms of γ, and MN or RON, using η_{qMN} or η_{qRON} depending on the kind of fuel. Also, maximum thermal efficiency by chemical composition could be estimated in terms of $\eta_{qH/C}$, relating to the availability to produce work of liquid and gaseous fuels.

The methodology proposed defines that exergy and entropy of fuels are correlated for EE generation at the KT with fuel´s T_{ad}, and η_{qT} or η_{Otto}. Besides, the exergy efficiency for Otto cycles

in SI engines for gaseous, and liquid fuels is based on η_{qT}, estimating the availability to produce work by the fuel´s energy quality (by the fuel´s physicochemical properties relative to methane), and limited by the fuel´s knocking resistance (MN).

Figure 10 presents exergy efficiency for liquid and gaseous fuels for Otto cycles. Liquid and gaseous fuels are ordered from left to right increasing RON or equivalent (RON~) beginning with n-heptane (RON0) and finishing with biogas (MN140/RON~171). According to the methodology for estimating exergy efficiency in SI engines, methane (RON~143) has the highest exergy efficiency (η_{qT}=54.1%) of all the fuels because it has the highest H/C ratio (4/1) combined with a high knocking resistance (MN100/RON~143). Fuel RON~141 has the second place with η_{qT}=53.7%, this fuel is a kind of biogas blend with 36% methane and 10% hydrogen (see table 3 in the appendix for fuel composition and main properties), and it exhibited high exergy efficiency due to its high MN97, and the increased H/C ratio due to the hydrogen addition, which improves fuel´s S_L, turbulent flame speed, and reduces heat losses to rise thermal efficiency and engine performance. Biogas B (RON~157) was 3rd with η_{qT}=53.6% because it has a good balance between chemical composition (80%CH_4/20%CO_2), H/C ratio, γ, and its high knocking resistance (MN120). RON147~ was 4th with η_{qT}=53.4%, this fuel is a biogas blend with 38% methane and 5% hydrogen, which exhibited high exergy efficiency due to its high MN105, and the increased H/C ratio due to the addition of hydrogen.

Biogas A (RON~171) is 5th with a typical chemical composition (60%CH_4/40%CO_2) with high η_{qT} (53.3%) due to it has the highest η_{qMN} =58.9% related with the highest knocking resistance (CCR=18:1 and MN140) of all the fuels, due to its high CO_2 concentration, but the CO_2 decreases the H/C ratio and reduces $\eta_{qH/C}$=47.7% which diminishes the averaged η_{qT}, also, this fuel requires high turbulence and pressure for combustion due to its low S_L and E_D.

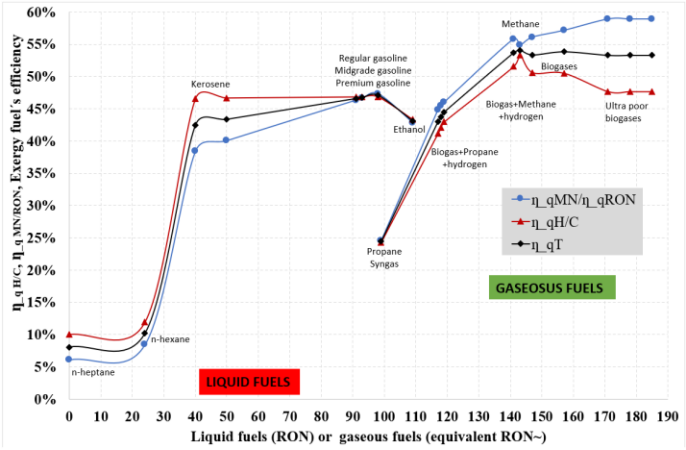

Figure 10 Fuel´s exergy efficiency (n_{qT}), n_{qMN}/ n_{qRON} vs. fuel's RON.

Premium gasoline is 6th with a high RON98, it has a good balance between H/C ratio and γ. Midgrade and regular gasoline are 7th and 8th, with RON93 and RON91, respectively, exhibiting lower knocking resistance than premium gasoline. Gaseous fuels (MN64/RON~117) and (MN65/RON~118), are blends of biogas with propane and hydrogen, are 9th and 10th respectively, due to their low γ, and medium knocking resistance due to the propane concentration and the hydrogen addition. A liquid renewable fuel as ethanol is 11th with the highest RON109 of liquid fuels, with a high H/C ratio but a lower γ (1.25). MN66/RON~119 is a fuel blend of biogas with propane, it is 12th with a low γ and a low H/C ratio. Kerosene A and B are 13th and 14th, both have a low RON50 and RON40 respectively, and low H/C ratios. Propane (MN37 RON~99) is 15th due to its low γ and the lowest MN of the gaseous fuels tested; in some countries, this fuel is used as fuel for engine cars to substitute gasoline (~RON) using engines with CR close to 9:1 with similar output power but with lower thermal efficiencies. n-hexane and n-heptane are the last 16th and 17th, with the lowest RONs of 24 and 0, as well as the lowest γ.

The methodology for the estimation of exergy efficiency allows the comparison of liquid and gaseous fuels. Gaseous fuels like biogases (MN120-MN140), and fuel blends of biogas with hydrogen (MN97 and MN105) are known as alternative fuels. These fuels have high equivalent RONs>135, resulting in higher exergy efficiency than the most common liquid fuels, such as gasoline (RONs between 91 and 98), ethanol (RON109), and kerosene (RON50 and RON40. Methane and alternative fuels exhibited to have higher octane, (~RON), and exergy efficiency than gasoline in SI engines. These fuels could be more powerful than oil-derived fuels because of their high knocking resistance and combustion properties. Also, methane and alternative fuels produce lower pollutant emissions due to their light chemical composition and low flame temperature. Methane and alternative fuels require lower air quantity for the combustion process as the E_D is lower than that of liquid fuels. T_{ad} for alternative fuels is lower than one of the oil-derived fuels, guaranteeing lower NO_x emissions. Gases have greater entropy than liquids, resulting that gaseous fuels have greater entropy than liquid fuels, and according to equation 15, gaseous fuels have greater exergy than liquid fuels in SI engines because they can be burnt at higher pressures and turbulence. The proposed methodology for SI engines concludes that the fuels that get combustion at the highest entropy (conditions of high pressure, temperature, and turbulence) without knocking are the fuels that have the highest exergy. The environmental and social impact of this study is that it positions biogases (renewable fuels) as the greatest potential exergy fuels operating in SI engines with high CR, seeking a paradigm shift. New proposals for future research are, presenting a theoretical-experimental model for the octane, entropy, and exergy of fuels in SI engines, and scaling the results for the design and conversion of a 50 kW diesel engine for biogas SI engine.

IV. CONCLUSIONS

It is proposed a novel methodology for estimating fuel`s exergy, and exergy efficiency in SI engines for liquid and gaseous fuels according to Otto cycles principles. η_{qT} for gaseous and liquid

fuels was defined, estimating the fuel's exergy efficiency based on the fuel´s chemical composition, but limited by the knocking resistance. The novelty of the methodology is based on the combination of two scientific methodologies, one to measure the fuel`s MN, and the other to estimate fuel`s energy quality. Also, it is included data from various fuels tested in CFR engines. The main conclusions of the research are as follows:

- According to the methodology presented, gaseous fuels have greater entropy and exergy than liquid fuels. To estimate exergy for Otto cycles in SI engines, the equation $\overline{X_f} = \eta_{qT} * S_f * T_{ad}$ is proposed to correlate octane, entropy and exergy. Fuels with the highest η_{qT} have the highest exergy due to their energy quality (high γ, H/C ratio, and low S_L, T_{ad}, E_D), also due to the highest knocking resistance (MN/RON), with the lowest pollutant emissions by the low T_{ad}, and lower consumption of oxygen from the atmosphere because of the low E_D.
- The unified methodology for estimating the exergy efficiency of liquid and gaseous fuel is a complete analysis of engine performance, considering the maximum thermal efficiency according to thermodynamics laws applied to the Otto cycles, and using the fuel´s knocking resistance as the engine performance limit.
- Fuels like biogases with high entropy in their chemical composition (due to the complex process of its production) have high exergy at the KT because of the high γ, low T_{ad}, low S_L, low E_D, and high knocking resistance (MN), despite the low H/C ratios; it agree with thermodynamics laws applied for the Otto cycles principles because biogases can be burnt at the highest CCR and turbulence intensities with high T_A and P_A.
- The combustion process at high compression pressures and high turbulence intensities results in high entropy of the system in-cylinder for high exergy release. Alternative fuels with high equivalent RONs (>135) have higher exergy efficiency than types of gasoline. Alternative fuels are cleaner with lower pollutant emissions and require less air for combustion due to the lower fuel´s E_D. Methane (MN100/RON~143) and biogases (RON~157-171) have higher exergy efficiency than gasoline (RON91-98), ethanol (RON109), and kerosene (RON50 and RON40). For liquid and gaseous fuels, higher octane represents higher exergy.
- η_{qT} is proposed for estimating the exergy efficiency of liquid and gaseous fuels, considering the fuel´s energy quality, evaluating two effects to determine the engine performance limit: fuel's chemical availability to produce work based on its physicochemical properties, H/C ratio, and limited by its knocking resistance measured with MN/RON.
- η_{Otto} and η_{qMN} are similar in values but were demonstrated that η_{qT} estimates better engine performance tendency for EE generation in the BSI engine at the KT. η_{qT} could predict the engine limit, it could help to improve engine design because of combustion conditions and the best physicochemical properties could be selected for the mixture of air and fuel, concluding that strategies of knocking suppression are the key to increase SI engine performance and reduce emissions.

ACKNOWLEDGMENTS

Bismillah, I would like to acknowledge the support granted by. 1. "Ministerio de Ciencia Tecnología e Innovación de Colombia" by the postdoctoral scholarship (2021). 2. Prociencia-Peru for financing the project "Theoretical and experimental research for the design and scaling of a generator set from 8 kW to 50 kW using a hybrid diesel engine in spark ignition mode for biogas and natural gas for bi-fuel operation, at the UTP-Peru" between 2022 and 2023.

V. REFERENCES

[1] J.B. Heywood. Internal Combustion Engines Fundamentals, ed. McGraw Hill 1988. Chapters 1 and 6.

[2] Department of applied physics. University of Seville. http://laplace.us.es/wiki/index.php/Ciclo_Otto_(GIE), Ciclo Otto (GIE), Date of the website consultation was 22/08/2022.

[3] G.A. Karim. The onset of knock in gas-fueled SI engines prediction and experiment. Journal of KONES Powertrain and Transport 2007,14(4), pp: 165-175.

[4] G. Shu, J. Pan, and H. Wei. Analysis of onset and severity of knock in SI engine based on in-cylinder pressure oscillations. Applied Thermal Engineering 2013, 51(2), pp: 1297-1306.

[5] B. Breaux, C. Hoops, and W. Glewen. The effect of in-cylinder turbulence on lean, premixed, spark-ignited engine performance. Journal of Engineering for Gas Turbines and Power 2016, 138, pp: 081504-081515.

[6] B.J. Bora, U.K. Saha, S. Chatterjee, V. Veer. Effect of compression ratio on performance, combustion and emission characteristics of a dual fuel diesel engine run on biogas. Energy Conversion and Management 2014, 87, pp: 1000-1009.

[7] D. Janecek, D. Rothamer, J. Ghandhi. Investigation of cetane number and octane number correlation under homogenous-charge compression-ignition engine operation. Proceedings of the Combustion Institute 36, Issue 3, 2017, pp: 3651-3657.

[8] G.A. Karim. Autoignition and Knock in Engines Fueled with Hydrogen and Hydrogen Supplemented Gaseous Fuel Mixtures. U.C. Mechanical Engineering 2007, Editor report.

[9] X. Yu, Z. Liu, and H. Dou. Optimize combustion of compressed natural gas engine by improving in-cylinder flows. International journal of automotive technology 2013, 14(4), pp: 539−549.

[10] M. Leiker, K. Christoph. Evaluation of antiknocking property of gaseous fuels by means of methane number and its practical application to gas engines. American Society of Mechanical Engineers 1972, 72: DGP-4.

[11] K.M Mardi, S. Khalilarya, and A. Nemati. A numerical investigation on the influence of EGR in a supercharged SI engine fueled with gasoline and alternative fuels. Energy Conversion and Management 2014, 83, pp: 260-269.

[12] K. Lee, T. Kim, H. Cha, S. Song, K. Min Chu. Generating efficiency and NOx emissions of a gas engine generator fueled with a biogas–hydrogen blend and using an exhaust gas recirculation system. International Journal of Hydrogen Energy 2010, 35(11), pp: 5723-5730.

[13] H. Li, G.A. Karim. Knock in SI hydrogen engines. International Journal of Hydrogen Energy 2004, 29, pp: 859-865.

[14] Y. Chen, R. Raine. A study on the influence of burning rate on engine knock from empirical data and simulation. Combustion and Flame 2015, 162, pp: 2108–2118.

[15] E. Porpatham, A. Ramesh, B. Nagalingam. Effect of hydrogen addition on the performance of a biogas fueled SI engine. International Journal of Hydrogen Energy 2007, 32(12), pp: 2057-2065.

[16] S. Kumar, N. Sahoo, and K. Mohanty. Comparative assessment of a SI engine fueled with gasoline and raw biogas. Renewable Energy 2019, 134, pp: 1307-1319.

[17] A. Arunachalam, and D.B. Olsen. Experimental evaluation of knock characteristics of producer gas. Biomass and Bioenergy 2012, 37, pp: 169-176.

[18] R. Chandra, V.K. Vijay, P.M. Subbarao, T.K. Khura. Performance evaluation of a constant speed IC engine on CNG, methane enriched biogas, and biogas. Applied Energy 2011, 88-11, pp: 3969-3977.
[19] X. Zhen, Y. Wang, S. Xu, Y. Zhu, C. Tao, T. Xu, and M. Song. The engine knock analysis – An overview. Applied Energy 2012, 91, pp: 628-636.
[20] M. Malenshek, and D.B. Olsen. Methane number testing of alternative gaseous fuels. Fuel 2009, 88, pp: 650-656.
[21] H.J. Schiffgens, H. Endres, H. Wackertapp, E. Schrey. Concepts for the adaptation of SI gas engines to changing methane number. Journal Engineering of Gas Turbine and Power 1994, 116, pp: 733-739.
[22] T.W. Ryan, T.J. Callahan, S.R. King. Engine knock rating of natural gases Methane Number, Journal Engineering of Gas Turbine and Power 1993, 115, pp: 769-776.
[23] V. Zimont. Gas Premixed Combustion at High Turbulence. Turbulent Flame Closure Model Combustion Model. Experimental Thermal and Fluid Science 2000, 21, pp: 179-186.
[24] E. Porpatham, A. Ramesh A, and B. Nagalingam. Effect of swirl on the performance and combustion of a biogas fueled SI engine. Energy Conversion and Management 2013, 75, pp: 224-233.
[25] V. Makarevicienea, E. Sendzikienea, S. Pukalskasb, and A. Rimkusb. Performance and emission characteristics of biogas used in diesel engine operation. Energy Conversion and Management 2013, 75, pp: 224-233.
[26] E. Porpatham, A. Ramesh A, and B. Nagalingam. Investigation on the effect of concentration of methane in biogas when used as a fuel for a SI engine. Fuel 2008, 87(9), pp: 1651-1659.
[27] T. Bond, M.R. Templeton. History and future of domestic biogas plants in the developing world. Energy for Sustainable Development 2011,15 (4), pp: 347-354.
[28] S. Patel, D. Tonges, D. Mahajan. Biogas potential on Long Island, New York: A quantification study. Journal of Renewable Sustainable Energy 2011, 3, pp: 043118-043128.
[29] J. Huang, R.J. Crookes. Assessment of simulated biogas as a fuel for the SI engine. Fuel 1998, 77 (15), pp: 1793-1801.
[30] C. Jeong, T. Kim, K. Lee, S. Song, K. Chun. Generating efficiency and emissions of a spark-ignition gas engine generator fueled with biogas–hydrogen blends. International Journal of Hydrogen Energy 2009, 34 (23), pp: 9620-9627.
[31] X. Kan, D. Zhou, W. Yang, X. Zhai, and C.H. Wang. An investigation on utilization of biogas and syngas produced from biomass waste in premixed SI engine. Applied Energy 2018, 212, pp: 210-222.
[32] Y. Kim, N. Kawahara, K. Tsuboi, and E. Tomita. Combustion characteristics and NOX emissions of biogas fuels with various CO2 contents in a micro co-generation spark-ignition engine. Applied Energy 2016, 182, pp: 539-547.
[33] S.R. Bell, S. Rathnam. Fuel composition effects on emissions from a spark-ignited engine operated on simulated biogases. Transactions of the ASME 2001, 123, pp: 132-138.
[34] J. Chulyoung, T. Kim, K. Lee, S. Song, K. Chun. Generating efficiency and emissions of a spark-ignition gas engine generator fueled with biogas–hydrogen blends. International Journal of Hydrogen Energy 2009, 34(23), pp: 9620-9627.
[35] P. Cheolwoong, S. Park, Y. Lee, C. Kim, S. Lee, Y. Moriyoshi. Performance and emission characteristics of a SI engine fueled by low calorific biogas blended with hydrogen. International Journal of Hydrogen Energy 2011, 36(16), pp: 10080-10088.
[36] J.P. Gómez Montoya, and A.A. Amell. Phenomenological Analysis of the Combustion of Gaseous Fuels to Measure the Energy Quality and the Capacity to Produce Work in Spark Ignition Engines. Journal of Engineering for Gas Turbines and Power 2021, 143 (1), pp: 0510161-05101612.
[37] J.P. Gómez Montoya, and A.A. Amell. Phenomenological analysis of the combustion of gaseous fuels to measure energy quality and capacity to produce work in SI engines, part 2. Journal of Engineering for Gas Turbines and Power, May 2022, 144(5), pp: 051002,14p.
[38] J.P. Gómez Montoya, A.A. Amell, and D.B. Olsen. Prediction and measurement of the critical compression ratio and methane number for blends of biogas with methane, propane, and hydrogen. Fuel 2016, 186, pp: 168-175.
[39] J.P. Gómez Montoya, A.A. Amell, and D.B. Olsen. Engine operation just above and below the KT using a blend of biogas and natural gas. Energy 2018, 153, pp: 719-725.
[40] J.P. Gómez Montoya, G. Amador, A.A. Amell, and D.B. Olsen. Strategies to improve the performance of a spark-ignition engine using fuel blends of biogas with natural gas, propane, and hydrogen. International Journal of Hydrogen Energy 2018, 43, pp: 21592 - 21602.
[41] J.P. Gómez Montoya, G. Amador, and A.A. Amell. Effect of equivalence ratio on knocking tendency in SI engines fueled with fuel blends of biogas, natural gas, propane, and H2. International Journal of Hydrogen Energy 2018, 43 (51), pp: 23041-23049.
[42] J.P. Gómez Montoya, and A.A. Amell. Effect of the turbulence intensity on knocking tendency in a SI engine with high compression ratio using biogas and blends with natural gas, propane, and hydrogen. International Journal of Hydrogen Energy 2019, 44, pp:18532-18544.
[43] J.P. Gómez Montoya, A.A. Amell, and D.B. Olsen. Operation of a SI engine with high CR using biogas blended with natural gas, propane, and hydrogen. Journal of Engineering for Gas Turbines and Power 2019, 141(5), pp: 051006-051016.
[44] G. Amador, L. Corredor, J.P. Gómez Montoya, and D.B. Olsen. Methane number measurements of hydrogen/carbon monoxide mixtures diluted with carbon dioxide for syngas spark ignited ICE applications. Fuel Journal 236 (2019), pp: 535–543.
[45] J. Kubesh, and S. King. Effect of gas composition on octane number of natural gas fuels. SAE Technical paper series 922359. International Fuels and Lubricants Meeting and Exposition San Francisco, California, October 19-22,1992. ISSN 01 48-71 91.
[46] A. Prakash, C. Wang, A. Janssen, A. Aradi, and R. Cracknell. Impact of fuel sensitivity (RON-MON) on engine efficiency. SAE Int. Journal Fuels Lubricants 2017, 10(1), doi:10.4271/2017-01-0799.
[47] A. García, J. Monsalve-Serrano, D. Villalta, and R. Sari. Octane number influence on combustion and performance parameters in a Dual-Mode Dual-Fuel engine. Fuel 258 (2019), pp: 116140.
[48] C. Druzgalski, S. Lapointe, R. Whitesides, and M. McNenly. Predicting octane number from microscale flame dynamics. Combustion and Flame 208 (2019), pp: 5–14.
[49] C. Rakopoulos, and E.G. Giakoumis. Second-law analyses applied to internal combustion engines operation. Progress in Energy and Combustion Science 2006, 32, pp: 2–47.
[50] V. Patil et al. Applicability of ketone-gasoline blended fuels for spark ignition engine through energy-exergy analyses. Fuel 339 (2023) 127416.
[51] T. Akbiyik et al. Energy and exergy analysis with emissions evaluation of a gasoline engine using different fuels. Fuel 345 (2023) 128189.
[52] X. Yu et al. Energy and exergy analysis of a combined injection engine using gasoline port injection coupled with gasoline or hydrogen direct injection under lean burn conditions. International Journal of Hydrogen Energy 46 (2021) 8253-8268.
[53] Yasin Sohret. Energy and exergy analyses of a hydrogen fueled SI engine: Effect of ignition timing and compression ratio. Energy 175 (2019) 410-422.
[54] C. Rakopoulos. Exergy evaluation of equivalence ratio, compression ratio and residual gas effects in variable compression ratio spark-ignition engine using quasi-dimensional combustion modeling. Energy, 244, Part B, 1 April 2022, 123080.
[55] B. Hong. Energy and exergy characteristics of an ethanol-fueled heavy-duty SI engine at high-load operation using lean-burn combustion. Applied Thermal Engineering 224 (2023) 120063.

V. APPENDIX

Table 1 Fuel´s MN/RON, composition, and properties.

Fuels MN/RON, chemical composition.	MN / MN~	RON/ RON~	γ=Cp/Cv	H/C ratio.	η_qMN/ η_qRON	η_qH/C	η_qT
MN140* (Biogas A) RON 171~	140	171	1.303	2.40	58.9%	47.7%	53.3%
MN120 (Biogas B) RON 157~	120	157	1.301	3.20	56.9%	50.3%	53.6%
MN105 (Biogas+CH4+H2 A) RON 147~	105	147	1.305	3.15	56.1%	50.6%	53.4%
MN100 (CH4) RON 143~	100	143	1.299	4.00	54.9%	53.3%	54.1%
MN97 (Biogas+CH4+H2 B) RON 141~	97	141	1.310	3.26	55.8%	51.6%	53.7%
MN66 (Biogas+C3H8) RON 119~	66	119	1.246	2.50	44.9%	41.2%	43.0%
MN65 (Biogas+C3H8+H2 A) RON 118~	65	118	1.251	2.58	45.4%	42.0%	43.7%
MN64 (Biogas+C3H8+H2 B) RON 117~	64	118	1.256	2.67	46.0%	43.0%	44.5%
MN37 C3H8 RON 99~	37	99	1.127	2.67	24.6%	24.3%	24.5%
RON 109 Ethanol (C2H5OH)	27	109	1.250	3.00	42.8%	43.4%	43.1%
RON 98 Premium gasoline	23	98	1.300	2.25	47.3%	46.9%	47.1%
RON 93 Midgrade gasoline	17	93	1.300	2.25	46.6%	46.9%	46.7%
RON 91 Regular gasoline (C8H18)	14	91	1.300	2.25	46.3%	46.9%	46.6%
RON 50 Kerosene A (C10H22)	- 39	50	1.300	2.20	40.0%	46.7%	43.4%
RON 40 Kerosene B (C12H26)	- 52	40	1.300	2.17	38.4%	46.6%	42.5%
RON 24 n-hexane (C6H14)	- 72	24	1.060	2.33	8.4%	12.0%	10.2%
RON 0 n-heptano (C7H16)	- 103	0	1.050	2.29	6.1%	10.0%	8.1%

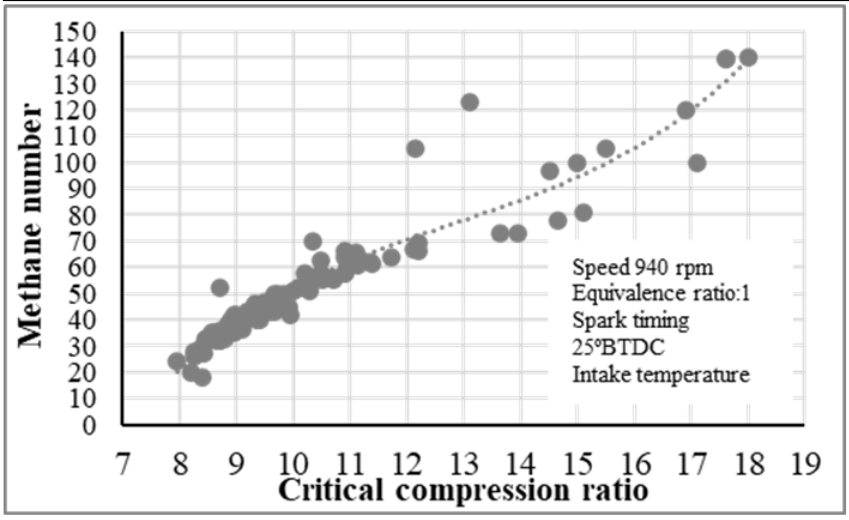

Figure 11 Correlation between fuel´s MN and CCR tested in CFR engine for gaseous fuels.

Table 2 List of acronyms.

Description	Acronym	Description	Acronym	Description	Acronym
Adiabatic flame temperature	T_{ad}	Hydrogen/Carbon ratio	**H/C**	Octane Number	**ON**
Biogas spark ignition	**BSI**	Indicated mean pressure	**IMEP**	Spark ignition	**SI**
Coefficient of variation	**COV**	knock peak pressure	**KPP**	Spark timing	**ST**
Computational Fluid Dynamics	**CFD**	Knocking threshold	**KT**	Top dead center	**TDC**
Cooperative fuel research	**CFR**	Laminar flame speed	S_L	Heat capacity ratio	γ
Crankshaft angle degrees	**CAD**	low heating value	**LHV**	Otto cycle efficiency	η_{Otto}
Critical compression ratio	**CCR**	Maximum electrical energy	$E_{E\ max}$	generating efficiency	η_g
Energy density	E_D	Methane number	**MN**		

Table 3 Fuel composition and main properties.

Blend designation (MN)	Blend composition	Blend properties			Laminar flame speed (cm/s), equivalence ratio of 0.9, 1 atm, and 25 °C
		LHV MJ/m³ fuel	Energy density MJ/m³ st air	Methane number	
140	100% Biogas (60/40 CH_4/CO_2)	20.35	3.44	140.0	23.57
120	100% Biogas (80/20 CH_4/CO_2)	27.14	3.57	120.0	30.22
105	57% Biogas + 38% Methane +5% H_2	25.00	3.58	105.3	30.32
100	100% Methane	34.55	3.58	87.2	34.98
97	54% Biogas + 36% Methane +10% H_2	24.22	3.59	96.5	31.74
66	83% Biogas + 17% Propane	31.98	3.64	65.8	32.83
65	79% Biogas + 16% Propane +5% H_2	30.89	3.65	65.2	33.91
64	75% Biogas + 15% Propane +10% H_2	30.71	3.77	63.8	34.95
37	100% Propane	94.10	3.73	37.1	43.50